

The GA module, a mobile albumin-binding bacterial domain, adopts a three-helix-bundle structure

Maria U. Johansson^{a,*}, Maarten de Chateau^b, Lars Björck^b, Sture Forsén^a, Torbjörn Drakenberg^a, Mats Wikström^a

^aDepartment of Physical Chemistry 2, Chemical Center, University of Lund, P.O.B 124, S-221 00 Lund, Sweden

^bDepartment of Cell and Molecular Biology, Section for Molecular Pathogenesis, University of Lund, P.O.B 94, S-221 00 Lund, Sweden

Received 31 July 1995; revised version received 11 September 1995

Abstract We present the first study of the secondary structure and global fold of an albumin-binding domain. Our data show that the GA module from protein PAB, an albumin-binding protein from the anaerobic bacterial species *Peptostreptococcus magnus*, is composed of a left-handed three-helix bundle. The helical regions were identified by sequential and medium range NOEs, values of NH-C^αH coupling constants, chemical shift indices, and the presence of slowly exchanging amide protons, as determined by NMR spectroscopy. In addition, circular dichroism studies show that the module is remarkably stable with respect to both pH and temperature.

Key words: Albumin binding; Circular dichroism; GA module; NMR; Protein PAB; Three-helix bundle

1. Introduction

A number of pathogenic bacterial species, and especially Gram-positive bacteria, bind various human plasma proteins (for references see [1,2]). Human serum albumin (HSA) and immunoglobulin (Ig) G are the two quantitatively dominating plasma proteins, and surface proteins interacting with these molecules are found in different bacterial species. The first of the HSA-binding proteins to be isolated was protein G of group C and G streptococci. Originally described as an IgG-binding protein [3,4], this molecule was later found to have separate binding sites also for HSA [5] located in its NH₂-terminal half [6]. Some strains of the anaerobic bacterial species *Peptostreptococcus magnus* also express Ig- or HSA-binding proteins [7,8]. The protein responsible for Ig-binding was named protein L and interacts with Ig light chains [9], whereas different HSA-binding proteins have been isolated from *P. magnus* [10–12]. Protein PAB (peptostreptococcal albumin-binding) represents one of these proteins and contains a region of 45 amino acid residues showing a high degree of homology (60% identity) to

the HSA-binding domains of protein G [11]. This protein G-related albumin-binding domain, the GA module, was found to have been shuffled from group C or G streptococci to HSA-binding strains of *P. magnus* by a transfer mechanism including a plasmid related to a conjugative plasmid of *Enterococcus faecalis*, thereby providing the first example of contemporary module shuffling [11]. So far, 16 GA modules have been identified in 6 proteins of 4 different bacterial species. The functional role of this mobile bacterial domain is not understood, but several observations suggest that it adds selective advantages to the bacteria and contributes to virulence and pathogenicity, and that the use of antibiotics has promoted the transfer of the GA module.

In the present work the GA module (amino acid residues 213–266 in the intact protein PAB, numbered 1–53 in this paper) was cloned and expressed in *E. coli* in amounts sufficient for detailed biophysical studies. Thus, NMR and CD analyses were used to determine the stability, secondary structure, and global fold of this widely spread module.

2. Materials and methods

2.1. Protein production

A clone expressing only the GA module gave a very low yield of protein. Thus a larger fragment of protein PAB, starting with the NH₂-terminal of the mature protein and with the GA module at the COOH-terminus, comprising residues 27 through 265, was expressed in *E. coli* [11]. Oligonucleotides RX1N (dGCTCAGGCGGCCCGGACGAACCCGGGGCACCCAA) and RX3C (dCAGCAGGTCCGACTTATTAAGCGTGTGCTTTAAATTCGTT) were generated and used in PCR with chromosomal DNA from *P. magnus* strain ALB8 as template in order to generate an insert for cloning. The PCR product was then subjected to restriction enzyme digestion and ligation to the high level expression vector pHD389 [13]. After transformation into competent *E. coli* JM109 cells the resultant clones were screened by PCR and for expression of HSA-binding peptides. Apart from the peptide of expected size, 30 kDa according to the construct, a 5 kDa peptide could be co-purified from the periplasmic preparation of the clone on HSA-Sepharose [11]. The NH₂-terminus of this protein was determined and shown to be TIDQW. This sequence starts with T213, being six residues upstream of the GA module at L219. Evidently *E. coli* has cleaved the protein between M212 and T213. This 5 kDa protein was then separated from the larger peptides on a FPLC-Superose 12 column (Pharmacia). The fractions containing the GA module were pooled, dialysed against water, and lyophilised. The material appeared as a single band at 5 kDa upon analysis by SDS/PAGE and the molecular mass was determined to 5,900 by ultracentrifugation. The HSA-binding capacity of the recombinant GA module was established by its affinity for HSA coupled to Sepharose, Immobeads (Bio-Rad, Richmond, CA, USA) and in Western blot experiments probing HSA with radiolabeled GA. The GA module was radiolabeled with ¹²⁵I using Bolton-Hunter reagent (Amersham Corp., Buckinghamshire, UK). Also in competitive binding experiments the binding of radiolabeled GA was inhibited by unlabeled protein PAB or GA.

*Corresponding author. Fax: (46) (46) 2224543.
E-mail: mariaj@freja.fkem2.lth.se

Abbreviations: CD, circular dichroism; COSY, *J*-correlated spectroscopy; 2Q, double quantum; GA, protein G-related albumin-binding; HSA, human serum albumin; Ig, immunoglobulin; NOE, nuclear Overhauser effects; NOESY, nuclear Overhauser enhancement spectroscopy; NMR, nuclear magnetic resonance; PAB, peptostreptococcal albumin-binding; PCR, polymerase chain reaction; R-COSY, relayed COSY; TOCSY, total correlation spectroscopy; *T*_m, transition midpoint of thermal denaturation.

2.2. CD measurements

CD spectra were recorded in the far ultraviolet region (250 – 190 nm) on a JASCO J-720 spectropolarimeter in 1 mm path length cells with a scan speed of 10 nm/min and using a thermostated cell holder. Measurements were performed on protein samples (10 μ M, determined by amino acid analysis) in the range pH 2–11. The contribution from the solvent (distilled water) was subtracted using the JASCO software. A melting curve was obtained by measuring the ellipticity at 222 nm when raising the temperature from 4°C to 95°C at a rate of 50°C/h. The program SELCON [14] was used to estimate the α -helix content.

2.3. NMR samples

NMR samples were prepared by dissolving the protein fragment in 0.5 ml of $^1\text{H}_2\text{O}$ containing 10% $^2\text{H}_2\text{O}$, for the lock signal, or, in 99.8% (99.98% in the exchange experiments) $^2\text{H}_2\text{O}$. All samples contained 0.02% NaN_3 to inhibit bacterial growth. The final protein concentration was 3–4 mM. Aliquots of diluted ^2HCl or NaOH were used to adjust the pH to 6.0 or 5.0. All pH values are electrode readings with no correction for the deuterium isotope effect.

2.4. NMR experiments

The experiments were carried out on either a General Electric Omega 500 or a Varian Unity 500 spectrometer, both operating at 500 MHz. Chemical shifts were referenced to the water signal, which was assigned a value of 4.75 ppm at 27°C.

The following spectra were recorded at 27°C at pH 6.0 in $^1\text{H}_2\text{O}$: 2QF-COSY [15], TOCSY (spin lock period 100 ms, [16,17]), NOESY ($\tau_m = 200$ ms, [18]), a series of NOESY spectra ($\tau_m = 50, 100, 150,$ and 200 ms) and a 2Q ($\tau = 30$ ms, [19,20]). At otherwise identical conditions, but at 37°C, 2QF-COSY, TOCSY (spin lock period 100 ms), and NOESY ($\tau_m = 200$ ms) were collected. A NOESY at 47°C at pH 6.0 in $^1\text{H}_2\text{O}$ was also recorded. At 27°C and 37°C at pH 5.0 in $^1\text{H}_2\text{O}$ the following spectra were acquired: COSY [21,22] R-COSY ($\tau = 30$ ms, only 27°C, [23]), TOCSY (spin lock period 50 ms) and NOESY ($\tau_m = 120$ (27°C) and 150 ms (37°C)). At 27°C at pH 5.0 in $^2\text{H}_2\text{O}$, the following experiments were performed: COSY, TOCSY (spin lock period 50 ms), NOESY ($\tau_m = 120$ ms). At the same conditions but at pH 6.0 a 2Q was obtained. A series of four NOESY (27°C, $\tau_m = 200$ ms, 256 t_1 increments of 32 transients with 2048 data points) spectra were recorded at 27°C and pH 5.0. The water resonance was suppressed by preirradiation of the water resonance and the carrier was set on the solvent resonance. Data sets typically consisted of 512 t_1 increments of 64 transients with 2048 data points in the acquisition dimension.

2.5. Data processing and data analysis

The data were processed and analysed on a Silicon Graphics Indigo² computer using the Felix program (Biosym Technologies, San Diego). Prior to Fourier transformation, the data were zero-filled once in the evolution dimension and multiplied by a window function (pure/shifted sine bell or sine bell squared in most cases) in both dimensions. A COSY spectrum in $^1\text{H}_2\text{O}$ was zero-filled to a final size of 1024 \times 4096 for greater digital resolution in ω_2 . Dihedral coupling constants, $^3J_{\text{HN}2}$, were measured in this spectrum using the in-house program MAGNE on a SUN SPARCclassic workstation.

3. Results

3.1. CD measurements

CD spectroscopy was used to investigate the stability of the GA module with respect to temperature and pH variations. The CD spectra, of which those of pH 2 and 11 are shown in Fig. 1A, indicate that the GA module has a rather unchanged secondary structure between pH 2–11. CD spectra of the GA module (pH 6) at 27°C and 95°C are also shown in Fig. 1A. Negative maxima at 207 and 222 nm, and a positive maximum at 192 nm establish the helical structure of the module. Using the program SELCON [14], to estimate the α -helical content, we found that the GA module contains about 60% and 27% α -helix at 27 and 95°C, respectively. According to NMR data the GA module contains 64% α -helix (see below) at 27°C and

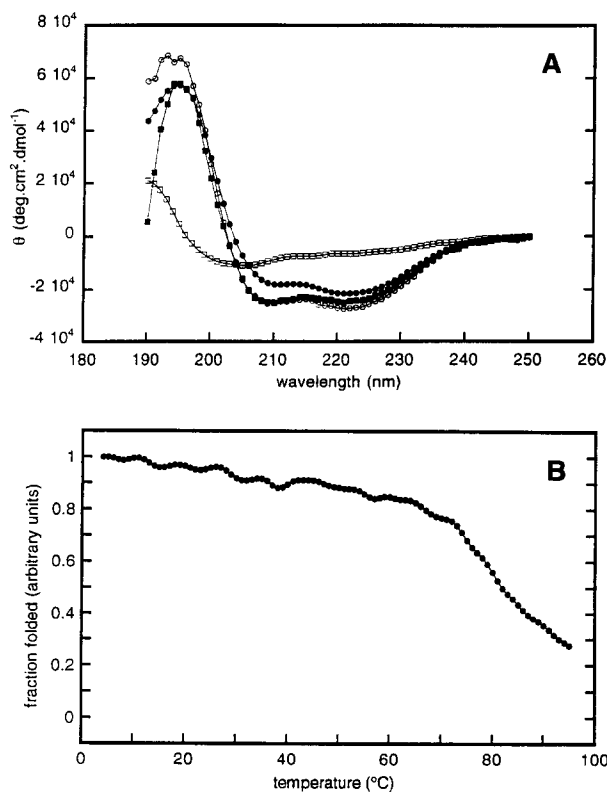


Fig. 1. Stability investigations of the GA module. (A) CD spectra recorded at various pH (27°C) and temperature values (pH 6.0; pH 2.0 (■), pH 11.0 (○), 27°C (●), and 95°C (□)). (B) Melting curve as obtained from CD data points (marked ●) at 222 nm and pH 6.

pH 6, which agrees well with the estimate above. Fig. 1B shows the melting curve recorded as mentioned earlier. The module starts to unfold above 70°C, but due to gradual unfolding over a large temperature range it was not possible to determine T_m , the transition midpoint of the thermal denaturation. The melting process seems reversible, since a CD spectrum recorded at 27°C, after heating to 95°C, was almost identical to a CD spectrum recorded at 27°C before increasing the temperature to 95°C (data not shown). The ellipticity at 222 nm was measured in the range 85 μ M to 1.3 mM, and was found to be linearly dependent on protein concentration (data not shown). Based on the above results the majority of our NMR experiments were performed at 27°C and pH 6.0.

3.2. Spin system identification

Spin systems were identified using a combination of the strategies described in [24,25]. Due to extensive overlap in some regions, spectra recorded at different combinations of pH and temperature had to be analysed. For example, eight residues have amide proton shifts between 8.07 and 8.10 ppm. The variations in chemical shifts due to temperature change were larger than those due to pH change (only amide proton resonances from Ala53 shifted significantly due to pH variations).

In the case of Glu40, only the NH/C^αH cross peak could be detected. The COSY cross peak was very weak, in spite of a large coupling constant (11 Hz), and the TOCSY cross peak was very broad. However, sequential $d_{\text{NN}}(i, i + 1)$ and

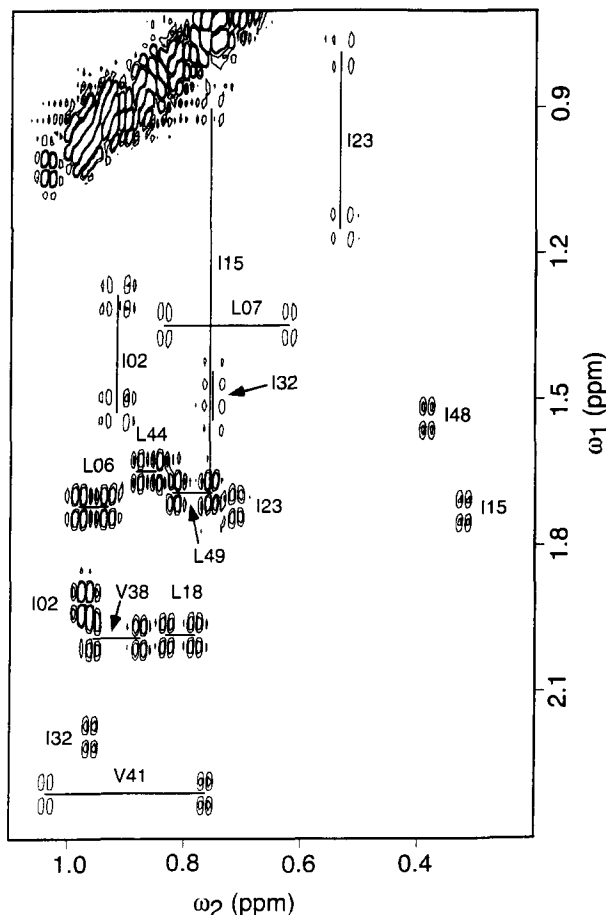


Fig. 2. Isoleucine/leucine/valine fingerprint region of a 2QF-COSY at 27°C, pH 6.0 ($^2\text{H}_2\text{O}$). The cross peaks are marked according to the sequential assignment ($\omega_1 = \text{C}^\beta\text{H}$, $\omega_2 = \text{C}^\gamma\text{H}_3$, and $\omega_1 = \text{C}^\gamma\text{H}$, $\omega_2 = \text{C}^\delta\text{H}_3$ for isoleucines, $\omega_1 = \text{C}^\gamma\text{H}$, $\omega_2 = \text{C}^\delta\text{H}_3$ for leucines, and $\omega_1 = \text{C}^\beta\text{H}$, $\omega_2 = \text{C}^\gamma\text{H}_3$ for valines). The two $\text{C}^\beta\text{H}/\text{C}^\delta\text{H}_3$ cross peaks for Ile48 are not shown due to overlap with the $\text{C}^\beta\text{H}/\text{C}^\gamma\text{H}_3$ cross peak of Ile23 (could be identified at 37°C) and due to overlap with the diagonal.

$d_{\alpha\text{N}}(i, i+1)$ cross peaks observed between Val41 and Glu40, and also between Glu40 and Glu39, made assignment of Glu40 possible. Nomenclature of sequential and medium range NOEs are taken from Wüthrich [24]. The NH proton resonance from the N-terminal residue, Thr1, was not visible, due to fast proton exchange.

According to the published sequence [11] the GA module should contain five leucines, four isoleucines and three valines. From the methyl region in the COSY (Fig. 2) and TOCSY spectra the five leucines could easily be identified, as could two valines. However, five and not four isoleucine spin systems could be identified. No unassigned cross peaks remained in the methyl region and therefore we assumed that there might be an error in the reported sequence (see below).

3.3. Sequential assignment

Sequential assignment was performed using the standard sequential assignment procedure [26]. During the sequential assignment we could identify residue 244 in the protein PAB gene to be an Ile (Ile32 in the GA module) and not a Val as reported earlier [11]. The reason for this error was an incorrect interpre-

tation of DNA sequencing data as confirmed by de Château (unpublished results). Fig. 3 summarises the connectivities seen during sequential assignment. The chemical shifts (27°C, pH 6.0) are available on request directly from the authors.

3.4. Secondary structure identification

The presence of strong sequential $d_{\text{NN}}(i, i+1)$, medium range $d_{\alpha\text{N}}(i, i+3)$, and $d_{\alpha\beta}(i, i+3)$ connectivities are indicative of helices. Other ways to delineate secondary structure elements, such as helices, from NMR data are by measurement of dihedral coupling constants, qualitative analysis of amide exchange rates, and by calculating chemical shift indices.

The torsion angle, ϕ , can be estimated from measurements of dihedral coupling constants, $^3J_{\text{HN}\alpha}$, using the Karplus equation [27]. A value of $^3J_{\text{HN}\alpha} < 5.5$ Hz corresponds to $100 > \phi > 20$ and a value of $^3J_{\text{HN}\alpha} > 8$ Hz corresponds to $-160 < \phi < -80$ (Fig. 3). Torsion angles within these ranges are indicative of helix and β -sheet structures, respectively. Coupling constants for certain residues were not possible to obtain, and other values were rejected due to large numerical uncertainty, as determined automatically within the MAGNE program.

Amide protons within helical regions, except the first three/four residues, are protected from exchange with solvent due to hydrogen bonding. To study the exchange rates of the amide protons four 4h NOESY spectra were recorded at 27°C, pH 5.0, starting 15 minutes after dissolving the sample in $^2\text{H}_2\text{O}$. Twenty-six residues were considered slowly exchanging since

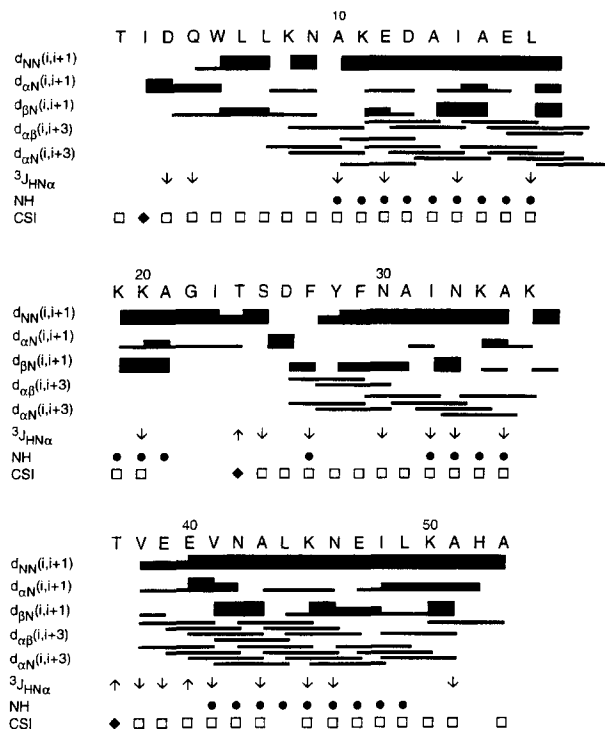


Fig. 3. Summary of the NMR data for the GA module at 27°C and pH 6. The intensities of the NOE cross peaks are indicated by the thickness of the line, classified as strong, medium, or weak. $^3J_{\text{HN}\alpha}$ measured as greater than 8.0 Hz or less than 5.5 Hz are indicated by up-arrow and down-arrow, respectively. Amide protons (NH) identified as exchanging slowly with solvent (\bullet) are indicated, as are chemical shift indices (CSI) of -1 (\square) and $+1$ (\blacklozenge).

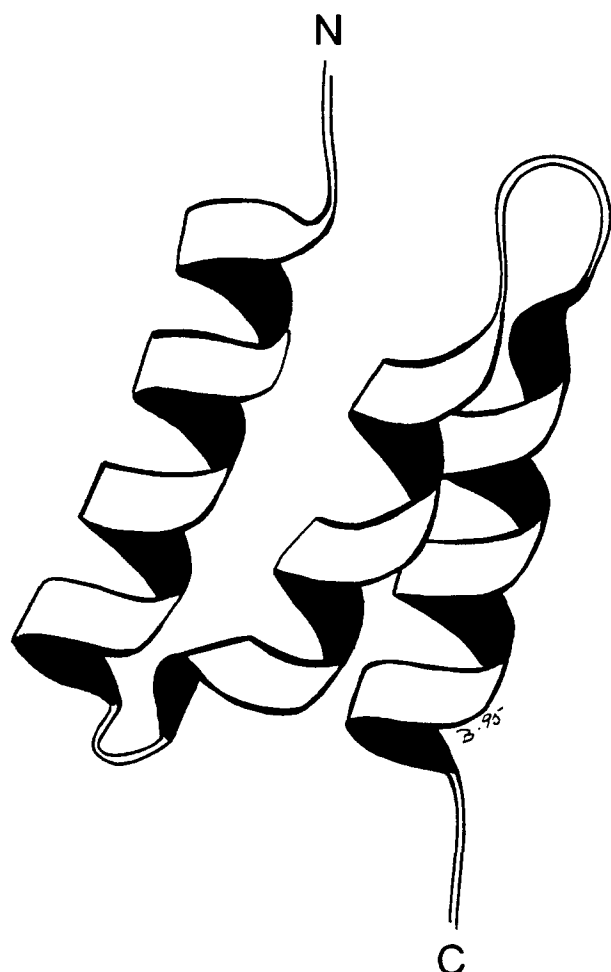


Fig. 4. Schematic view of the global fold of the three-helix bundle based on the NMR data summarised in Fig. 3.

they were not fully exchanged 15 minutes after addition of $^2\text{H}_2\text{O}$ (Fig. 3). Fourteen residues had a very slow exchange rate as they did not exchange fully within several days after dissolution of the sample in $^2\text{H}_2\text{O}$. Very slow exchange rates were observed primarily for residues in helix I, probably due to reduced flexibility and less exposure to solvent.

^1H NMR chemical shifts are strongly dependent on the nature of protein secondary structure [28]. The ^1H NMR chemical shift of C^αH is lower than the random coil value when in a helical conformation, and higher than the random coil value when in a β -strand extended conformation. The calculated chemical shift indices [29] are shown in Fig. 3.

Using all the above criteria we find that the GA module is a mostly helical protein with no β -structure. The helices may be identified as follows: helix I ranges from residues 7 or 8 to 20 or 21, helix II ranges from residues 26 to 35 or 36, and helix III ranges from residues 38 to 51. The large spin coupling for residue 40 is indicative of a kink in the helix, or that helix III does not start until residue 41. This will then also result in two turns, residue 21 to 25 and 36 to 40, respectively. In total, 34 out of 53 residues (60%) are involved in α -helices.

3.5. Global fold

The short linkers between the helices result in very little

flexibility in the global fold. This three-helix bundle must thus have the middle helix antiparallel to the other two which was verified by the presence of certain long range NOEs. Long range NOEs were seen between Leu7 (immediately preceding helix I) and Thr37 (in the loop between helices II and III), and also between Leu18 (in the C-terminal part of helix I) and Phe29 (in the N-terminal part of helix II). In addition, long range NOEs could be identified between Tyr28 (in the N-terminus of helix II) and Ile48 (at the end of helix III) and between Ala35 (at the C-terminus of helix II) and Val41 (in the N-terminus of helix III). Finally, it could be seen that helices I and III are in close spatial proximity, as indicated by long range NOEs between Ile23 (in the loop between helices I and II) and Ile 48, and also between Lys11 (in the N-terminus of helix I) and Val41. A majority of the long range NOEs appear between hydrophobic residues, which seem to form a hydrophobic core in the interior of the bundle. A schematic view of the global fold of the GA module is shown in Fig. 4.

4. Discussion

Several variations on the three-helix-bundle theme have been seen during recent years. Our results indicate that the three-helix-bundle of the GA module has a left-handed folding topology. This type of fold is also seen in the repetitive segments of spectrin [30], the IgG-binding domains of protein A from *Staphylococcus aureus* [31], an acyl-coenzyme A binding protein [32], and different pheromone proteins [33–35].

It is generally observed that proteins with high sequence identities have similar three-dimensional structures. It therefore appears likely that the various GA modules, e.g. in protein G, will be found to have similar three-dimensional structures, due to their high sequence identities (around 60%). The present work and previous investigations focused on bacterial surface proteins, underline the difficulties in relating secondary and tertiary structures to binding properties. Similar binding properties do not imply structural similarity. For instance, the Ig-binding domains of staphylococcal protein A and streptococcal protein G show no sequence homology and have very different global folds, but still bind to overlapping sites in IgG [36,37]. Neither does structural similarity imply similar binding characteristics. For example, protein A shows no affinity for HSA, but the fold of its IgG-binding domains [31,38] is strikingly similar to that of the GA module of protein PAB; i.e. a three-helix bundle with a left-handed folding topology. Another example is the IgG-binding domains of proteins L and G, which are both composed of a central α -helix packed against a four-stranded β -sheet [39–41], but interact with completely different sites in IgG [9]. The sequences in both examples are unrelated.

Apart from proteins containing the GA module also other bacterial surface proteins have been reported to interact with HSA. *Streptococcus pyogenes* is one of the most significant pathogens in humans. These bacteria express M proteins which are important virulence factors due to their antiphagocytic property (for references see [42]). Many members of the M protein family have homologous repeats located in the COOH-terminal half of the molecule. These so-called C repeats have recently been found to bind HSA [36,43,44]. Whether or not the binding of HSA contributes to the antiphagocytic property is not known. Like the GA modules the C repeats comprise about 40 amino acid residues, but these HSA-binding units show no

sequence homology. Nevertheless, they compete for the same binding site in HSA [36]. These observations indicate that HSA-binding in Gram-positive bacteria has evolved convergently which, in turn, suggests that the ability of binding this abundant plasma protein adds selective advantages to the bacteria. Whether this case of convergent evolution, in contrast to the IgGfc-binding regions of proteins A and G mentioned above, is reflected in three-dimensional similarities between the GA module and the C repeats, is currently being investigated.

Acknowledgements: This work was supported by the Swedish Research Council for Engineering Sciences (Grant 123) and the Swedish Medical Research Council (Grant 10434). The 500 MHz NMR spectrometer was purchased with grants from the Knut and Alice Wallenberg Foundation and the Swedish Council for Planning and Coordination of Research. The Swedish NMR Center is acknowledged for the use of the Varian Unity 500 spectrometer, and Birgitta Jönsson for the artwork in Fig. 4.

References

- [1] Boyle, M.D.P. (Ed.) (1990) *Bacterial Immunoglobulin Proteins*, Academic Press, San Diego.
- [2] Kehoe, M.A. (1994) *New Comp. Biochem.* 27, 217–261.
- [3] Björck, L. and Kronvall, G. (1984) *J. Immunol.* 133, 969–974.
- [4] Reis, K.J., Ayoub, E.M. and Boyle, M.D.P. (1984) *J. Immunol.* 132, 3091–3097.
- [5] Björck, L., Kastern, W., Lindahl, G. and Widebäck, K. (1987) *Mol. Immunol.* 24, 1113–1122.
- [6] Åkerström, B., Nielsen, E. and Björck, L. (1987) *J. Biol. Chem.* 262, 13388–13391.
- [7] Myhre, E. and Erntell, M. (1985) *Mol. Immunol.* 22, 879–885.
- [8] Myhre, E.B. (1984) *J. Med. Microbiol.* 18, 189–195.
- [9] Björck, L. (1988) *J. Immunol.* 140, 1194–1197.
- [10] Lämmler, C., Alaboudi, A. and Hildebrand, A. (1989) *Can. J. Microbiol.* 35, 614–618.
- [11] de Château, M. and Björck, L. (1994) *J. Biol. Chem.* 269, 12147–12151.
- [12] Murphy, J.P., Duggleby, C.J., Atkinson, M.A., Trowern, A.R., Atkinson, T. and Goward, C.R. (1994) *Mol. Microbiol.* 12, 911–920.
- [13] Dalbøge, H., Bech Jensen, E., Töttrup, H., Grubb, A., Abrahamson, M., Olafsson, I. and Carlsen, S. (1989) *Gene* 79, 325–332.
- [14] Sreerama, N. and Woody, R.W. (1993) *Anal. Biochem.* 209, 32–44.
- [15] Rance, M., Sorensen, O.W., Bodenhausen, G., Wagner, G., Ernst, R.R. and Wüthrich, K. (1985) *Biochem. Biophys. Res. Commun.* 131, 1094–1102.
- [16] Braunschweiler, L. and Ernst, R.R. (1983) *J. Magn. Reson.* 53, 521–528.
- [17] Bax, A. and Davis, D.G. (1985) *J. Magn. Reson.* 65, 355–360.
- [18] Macura, A. and Ernst, R.R. (1980) *Mol. Phys.* 41, 95–117.
- [19] Braunschweiler, L., Bodenhausen, G. and Ernst, R.R. (1983) *Mol. Phys.* 48, 535–560.
- [20] Levitt, M. and Freeman, R. (1979) *J. Magn. Reson.* 33, 473–476.
- [21] Marion, D. and Wüthrich, K. (1983) *Biochem. Biophys. Res. Commun.* 113, 967–974.
- [22] States, D.J., Haberkorn, R. and Ruben, D. (1982) *J. Magn. Reson.* 55, 151–156.
- [23] Wagner, G. (1983) *J. Magn. Reson.* 55, 151–156.
- [24] Wüthrich, K. (1986) *NMR of Proteins and Nucleic Acids*, Wiley, New York.
- [25] Chazin, W.J., Rance, M. and Wright, P.E. (1988) *J. Mol. Biol.* 202, 603–622.
- [26] Billeter, M., Braun, W. and Wüthrich, K. (1982) *J. Mol. Biol.* 155, 321–346.
- [27] Karplus, M. (1963) *J. Am. Chem. Soc.* 85, 2870–2871.
- [28] Wishart, D.S., Sykes, B.D. and Richards, F.M. (1991) *J. Mol. Biol.* 222, 311–333.
- [29] Wishart, D.S., Sykes, B.D. and Richards, F.M. (1992) *Biochemistry* 31, 1647–1651.
- [30] Yan, Y., Winograd, E., Viel, A., Cronin, T., Harrison, S.C. and Branton, D. (1993) *Science* 262, 2027–2030.
- [31] Gouda, H., Torigoe, H., Saito, A., Sato, M., Arata, Y. and Shimada, I. (1992) *Biochemistry* 31, 9665–9672.
- [32] Andersen, K.V. and Poulsen, F.M. (1992) *J. Mol. Biol.* 226, 1131–1141.
- [33] Brown, L.R., Mronga, S., Bradshaw, R.A., Ortenzi, C., Luporini, P. and Wüthrich, K. (1993) *J. Mol. Biol.* 231, 800–816.
- [34] Mronga, S., Luginbühl, P., Brown, L.R., Ortenzi, C., Luporini, P., Bradshaw, R.A. and Wüthrich, K. (1994) *Protein Science* 3, 1527–1536.
- [35] Ottiger, M., Szyperski, T., Luginbühl, P., Ortenzi, C., Luporini, P., Bradshaw, R.A. and Wüthrich, K. (1994) *Protein Science* 3, 1515–1526.
- [36] Frick, I.-M., Åkesson, P., Cooney, J., Sjöbring, U., Schmidt, K.-H., Gomi, H., Hattori, S., Tagawa, C., Kishimoto, F. and Björck, L. (1994) *Mol. Microbiol.* 12, 143–151.
- [37] Sauer-Eriksson, A.E., Kleywegt, G.J., Uhlén, M. and Jones, T.A. (1995) *Structure* 3, 265–278.
- [38] Torigoe, H., Shimada, I., Saito, M., Sato, M. and Arata, Y. (1990) *Biochemistry* 29, 8787–8793.
- [39] Gronenborn, A.M., Filpula, D.R., Essig, N.Z., Achari, A., Whitlow, M., Wingfield, P.T. and Clore, G.M. (1991) *Science* 253, 657–661.
- [40] Wikström, M., Sjöbring, U., Kastern, W., Björck, L., Drakenberg, T. and Forsén, S. (1993) *Biochemistry* 32, 3381–3386.
- [41] Wikström, M., Drakenberg, T., Forsén, S., Sjöbring, U. and Björck, L. (1994) *Biochemistry* 33, 14011–14017.
- [42] Fischetti, V.A. (1989) *Clin. Microbiol. Rev.* 2, 285–314.
- [43] Åkesson, P., Schmidt, K.-H., Cooney, J. and Björck, L. (1994) *Biochem. J.* 300, 877–886.
- [44] Retnoningrum, D.S. and Cleary, P.P. (1994) *Infect. Immun.* 62, 2387–2394.